

Relativistic graphene ratchet on semidisk Galton board

L.Ermann and D.L.Shepelyansky

¹ Laboratoire de Physique Théorique du CNRS, IRSAMC, Université de Toulouse, UPS, F-31062 Toulouse, France

² <http://www.quantware.ups-tlse.fr>

Dated: October 21, 2010; Revised: November 17, 2010

Abstract. Using extensive Monte Carlo simulations we study numerically and analytically a photogalvanic effect, or ratchet, of directed electron transport induced by a microwave radiation on a semidisk Galton board of antidots in graphene. A comparison between usual two-dimensional electron gas (2DEG) and electrons in graphene shows that ratchet currents are comparable at very low temperatures. However, a large mean free path in graphene should allow to have a strong ratchet transport at room temperatures. Also in graphene the ratchet transport emerges even for unpolarized radiation. These properties open promising possibilities for room temperature graphene based sensitive photogalvanic detectors of microwave and terahertz radiation.

PACS. 81.05.ue Graphene – 73.50.-h Electronic transport phenomena in thin films – 72.40.+w Photoconduction and photovoltaic effects – 05.45.Ac Low-dimensional chaos

Graphene [1] is a new two-dimensional material with a variety of fascinating physical properties (see e.g. [2]). One of them is a relativistic dispersion law for electron dynamics with an effective “light” velocity $s \approx 10^8 \text{cm/s}$ [3], another is a high mobility at room temperature which in suspended graphene reaches $\mu \approx 200,000 \text{cm}^2/Vs$ [4, 5, 6]. Our theoretical studies predict that these properties lead to emergence of a strong photogalvanic effect induced by radiation at room temperature in a semidisk antidot array placed in graphene plane. Such samples can function as a new type of room temperature sensors of microwave and terahertz radiation.

Ratchet transport, induced in asymmetric systems by *ac*-driving with zero mean force, attracted a significant interest of scientific community in view of various biological applications of Brownian motors [7, 8, 9]. Experimental observations of electron ratchet transport in asymmetric antidot arrays in semiconductor heterostructures have been reported in [10, 11, 12, 13]. A detailed theory of ratchet transport of 2DEG on semidisk Galton board was developed in [14, 15] for noninteracting electrons, and it was shown that the effect remains even in presence of strong interactions [16]. The theoretical predictions on polarization dependence have been confirmed in recent experiments [13]. According to theory [14, 15] the velocity of ratchet flow, induced by monochromatic linear polarized microwave force $\mathbf{f} \cos \omega t$ with a frequency ω , has a polarization dependence:

$$(\bar{v}_x, \bar{v}_y) = C_F V_F (f r_d / E_F)^2 (-\cos(2\theta), \sin(2\theta)), \quad (1)$$

where θ is an angle between the polarization direction and x -axis of semidisk array shown in Fig. 1, f is amplitude

of microwave force, V_F , E_F are Fermi velocity and energy, and C_F is a numerical factor depending on the ratio of periodic cell size R to semidisk radius r_d . In the limit of low density of semidisks with $R \gg r_d$ the theory [15] gives $C_F \propto (\ell_s / r_d)^2 / (1 + (\omega \ell_s / V_F)^2)$, with $\ell_s \sim R^2 / r_d \gg \ell_i$, where ℓ_i is the mean free path related to impurity scattering. The typical parameters of experiment [13] are $f/e \sim 1 \text{V/cm}$, $r_d \sim 1 \mu\text{m}$, $R/r_d \approx 4$, electron density $n_e \approx 2.5 \cdot 10^{11} \text{cm}^{-2}$ with $V_F \approx 2.2 \cdot 10^7 \text{cm/s}$, $E_F \approx 100 \text{K}$. For these conditions we have $f r_d / E_F \approx 1/100$, $C_F \approx 0.4$, so that the velocity of ratchet flow remains relatively small but well visible experimentally. Experimental data confirm the linear dependence of ratchet current on microwave power [13]. The relation (1) assumes that $\omega r_d / V_F < 1$ and that the mean free path ℓ_i remains larger semidisk size. For $\ell_i < r_d$ the array asymmetry disappears due to disorder scattering and ratchet velocity goes to zero.

The theory (1) assumes the usual quadratic dispersion law for electron dynamics $E = p^2 / 2m$, while graphene has a linear relativistic dispersion $E = sp$, so that such a case requires a separate analysis. Recently rectification and photon drag in graphene started to attract experimental [19] and theoretical interest [20, 21, 22]. We note that a case of relativistic dispersion appears for a flux quantum in long annular Josephson junction, which has been studied theoretically and experimentally in [23, 24], but there the dynamics takes place in 1D while for graphene it is essentially 2D. In addition, experiments with accelerator beams in crystals [25] show that a crystallographic potential creates an efficient channeling of relativistic particles. This gives some indication on a possible enhancement of

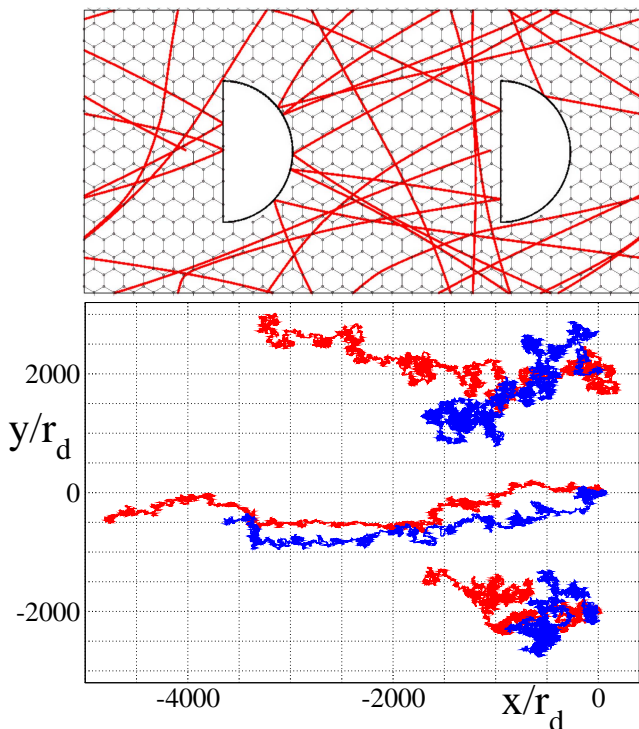


Fig. 1. (Color online) Top panel shows one electron trajectory on semidisk Galton square board (with periodic boundary conditions for two cells, no impurities, time $t \approx 100r_d/s$ and $fr_d/E_F = 0.05$), graphene structure is shown in a schematic way. Bottom panel shows two ratchet trajectories on a longer time for graphene (with initial conditions $(x, y) = (0, 2000)$ and $t \approx 2 \times 10^5 r_d/s$), model graphene (with $(x, y) = (0, 0)$ and $t \approx 10^5 r_d/s$) and 2DEG (with $(x/r_d, y/r_d) = (0, -2000)$ and same t) all of them at the same p_F and $T/E_F = 0.02$; here $R/r_d = 4$, $\theta = 0$, $\omega r_d/s = 0.5$, $V_F/s = 2$, and $fr_d/E_f = 0.1$ (red/gray curve), 0.025 (blue/black curve); impurity parameters are $s\tau_i/r_d = 5$, $\alpha_i = \pi/10$.

ratchet transport of electrons in graphene with a periodic array of asymmetric antidots.

The dynamics of electron on a 2D semidisk Galton board, shown in Fig. 1, is described by the Newton equations

$$\begin{aligned} d\mathbf{p}/dt &= \mathbf{f} \cos \omega t + \mathbf{F}_s + \mathbf{F}_i, \\ dr/dt &= s\mathbf{p}/|\mathbf{p}| \text{ (graphene)}; \quad d\mathbf{r}/dt = \mathbf{p}/m \text{ (2DEG)}, \end{aligned} \quad (2)$$

where the second equation corresponds to a relativistic case (l.h.s.) or to a non-relativistic case with an effective mass m (r.h.s.). Here the force \mathbf{F}_s describes elastic collisions with semidisks and \mathbf{F}_i models impurity scattering on a random angle ϕ_i ($|\phi_i| \leq \alpha_i$) with an effective scattering time τ_i .

Following [14], we use the Monte Carlo simulations with the Metropolis algorithm which keeps noninteracting electrons at the Fermi-Dirac distribution with fixed Fermi energy E_F and temperature T . As discussed in [14, 15, 16], in a wide range, a variation of energy equilibrium relaxation time τ_{rel} does not influence the ratchet velocity $\bar{\mathbf{v}}$. The later is computed along one or few very long trajectories with times up to $t = 10^8 r_d/s$. With this approach

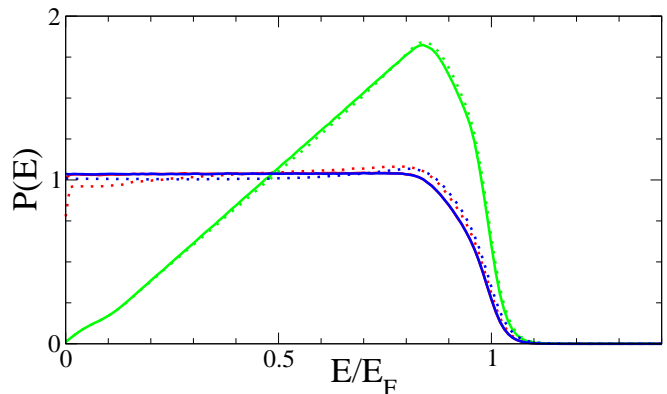


Fig. 2. (Color online) Dimensionless energy distribution functions $P(E)$ obtained numerically for 2DEG (blue/black curves), model graphene (red/gray curves) and graphene (green/gray curves). Parameters are kept as in Fig. 1 with $t \approx 10^7 r_d/s$ and temperature fixed to $T/E_F = 0.02$ with $fr_d/E_F = 0.02$ for full curves, and $fr_d/E_F = 0.1$ for dotted curves (full red and blue curves are overlapped).

we consider three cases of steady-state distributions. For 2DEG the phase volume is proportional to $pdp \sim mdE$, where E is an electron energy, hence here the probability distribution over energy is $P(E) = E_F dW/dE = \rho_{FD}(E)$ where $\rho_{FD}(E) = 1/(1 + \exp((E - E_F)/T))$ is the Fermi-Dirac distribution at temperature T . For graphene we have the phase volume $pdp \sim EdE/s^2$ so that the energy distribution has the form $P(E) = E_F dW/dE = B\rho_{FD}(E)E/E_F$, where B is a numerical normalization constant. We also consider a case of model graphene with the energy distribution being the same as for 2DEG with $P(E) = E_F dW/dE = \rho_{FD}(E)$ while the dynamical equations of motion correspond to the graphene spectrum. Typical examples of the steady-state distribution $P(E)$ in energy are shown in Fig. 2 for three models we consider: graphene, model graphene and 2DEG.

We note that the triangular lattice of disks had been used already by Galton [17] to demonstrate an emergence of statistical laws in deterministic systems. According to the mathematical results of Sinai [18] the dynamics is fully chaotic also for semidisk lattice used here (in absence of impurities, microwave driving and Metropolis thermostat).

A typical example of trajectory for graphene is shown in Fig. 1. The dynamics is clearly chaotic on one cell scale, while on large scale it shows diffusion and ratchet transport directed along x -axis. The ratchet displacement is significantly larger for model graphene compared to usual 2DEG with approximately the same parameters. Even more striking a decrease of the driving force by a factor 4 gives a significantly smaller reduction of the ratchet displacement compared to factor 16 expected from the theory for 2DEG (1). Thus for the model graphene the relativistic graphene ratchet has a strong enhancement compared to the usual 2DEG case studied before. The case of graphene has more strong ratchet compared to 2DEG but it is less strong compared to the model graphene.

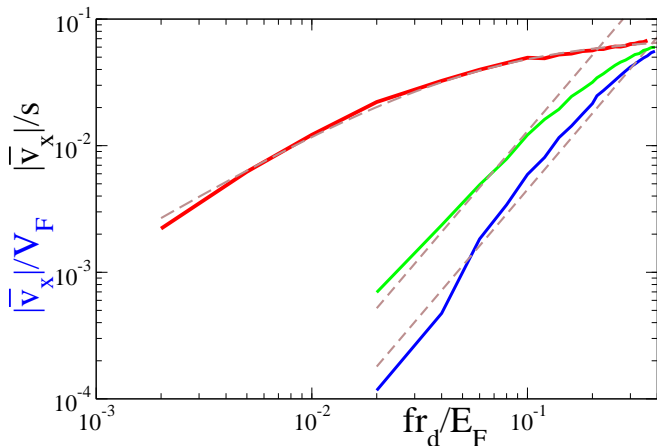


Fig. 3. (Color online) Rescaled ratchet velocity $|\bar{v}_x|$ as a function of rescaled force fr_d/E_F at polarization $\theta = 0$ for graphene (green/gray curve), model graphene (red/gray curve) and 2DEG (blue/black curve); when f is changing the system parameters are kept as Fig. 1. The bottom straight dashed line shows the fit dependence for 2DEG (3), the top dashed curve shows the fit dependence for model graphene (4) and the middle straight dashed line shows the fit dependence for graphene (5).

Detailed analysis of this enhancement and comparison of ratchet transport for graphene, model graphene and 2DEG, as a function of microwave driving force, are shown in Fig. 3. We fix $V_F/s = 2$ choosing p_F to be the same for graphene and 2DEG that corresponds to the same electron density n_e . For 2DEG the velocity of ratchet drops quadratically with force and is well described by the dependence

$$|\bar{v}_x|/V_F = C_F(fr_d/E_F)^2, \quad C_F = 0.45, \quad (3)$$

thus being in a good agreement with numerical data and theory presented in [14, 15, 16]. In a case of model graphene the field dependence is strikingly different and can be approximately described by the equation

$$|\bar{v}_x|/s = C_{g1}fr_d/(E_F + C_{g2}fr_d), \quad C_{g1} = 1.39, C_{g2} = 18.87. \quad (4)$$

According to Fig. 3 and Eqs. (3),(4) we have the enhancement factor for model graphene of approximately 100 and 10^3 at $fr_d/E_F = 0.02$ and 0.002 respectively.

However, for graphene we find approximately quadratic field dependence with

$$|\bar{v}_x|/s = C_g(fr_d/E_F)^2, \quad C_g = 1.3, \quad (5)$$

formal fit gives a power exponent 1.8 being close to 2. Thus in this case the ratchet velocity is comparable with the one of 2DEG.

Data presented for model graphene in the top panel of Fig. 4 show that the ratchet velocity is only weakly affected by increase of temperature T , which can become comparable with E_F , if the rate of impurity scattering is kept fixed. This is in agreement with the known results for 2DEG [14, 15]. An increase of impurity scattering (increase

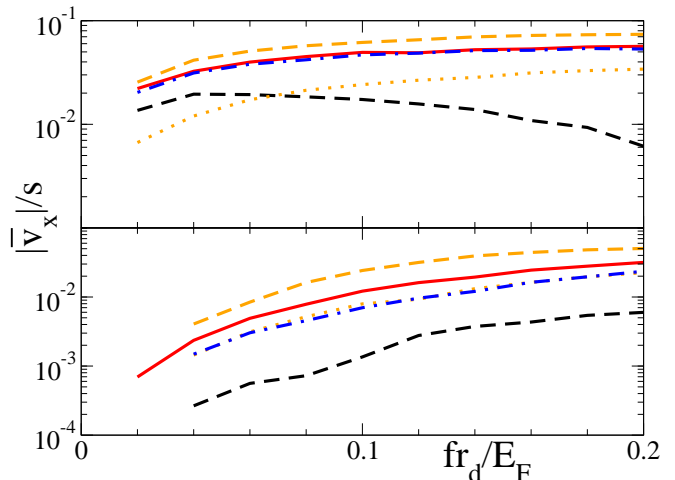


Fig. 4. (Color online) Rescaled ratchet velocity $|\bar{v}_x|$ as a function of rescaled force fr_d/E_F at polarization $\theta = 0$ for model graphene in top panel, and graphene in bottom panel, for the same values given in Fig. 1 with modifications of frequency, temperature or impurity scattering angle. Dashed orange/gray curves are for $\omega r_d/s = 0.25$, $T/E_F = 0.05$, $\alpha_i = \pi/10$; solid red/gray curves are for $\omega r_d/s = 0.5$, $T/E_F = 0.05$, $\alpha_i = \pi/10$ (Fig. 3 case); dotted-dashed blue/black line are for $\omega r_d/s = 0.5$, $T/E_F = 0.3$, $\alpha_i = \pi/10$; dotted orange/gray curves are for $\omega r_d/s = 0.5$, $T/E_F = 0.05$, $\alpha_i = \pi$; dashed black curves are for $\omega r_d/s = 0.1$, $T/E_F = 0.05$, $\alpha_i = \pi/10$.

of α_i) gives a reduction of \bar{v}_x but still the dependence on f remains approximately linear for $fr_d \ll E_F$. A decrease of frequency gives only a slight increase of \bar{v}_x for $\omega r_d/s \leq 0.5$ while for $\omega r_d/s \geq 1$ we start to see a drop of \bar{v}_x with ω . Such a dependence is in agreement with general theory [15] according to which the ratchet velocity is independent of frequency for $\omega r_d/s \ll 1$ and drops with frequency for $\omega r_d/s \gg 1$. It is interesting to note that at $\omega r_d/s = 1$ the velocity \bar{v}_x starts to decrease at large f . We will discuss this point later. For the graphene case the dependence of rescaled force f is shown in the bottom panel of Fig. 4 at same parameters. Here for all cases the velocity of ratchet increases with f , it is smaller compared to the case of model graphene in the top panel.

The polarization dependence of ratchet flow is shown in Fig. 5 for 2DEG and graphene; for 2DEG and model graphene the polarization dependence is shown in Fig. 6. For 2DEG the dependence is close to those of Eq. (1) being in agreement with previous studies [14, 15, 16]. A similar polarization dependence is present also for graphene. In contrast to that for model graphene the dependence on θ is not purely harmonic and appearance of flat domains near velocity maxima is well visible. In part the origin of this fluttering can be understood from the picture of average flow inside one periodic cell shown in Fig. 7. While for $\theta = 0$ the flow is relatively regular, for $\theta = 5\pi/32$ there is emergence of vortices that may be at the origin of fluttering in Fig. 6. It is clear that a theoretical description of such a vortex flow is a challenging task for further studies. We note that in agreement with theory [15] the polarization dependence on temperature is rather weak. It

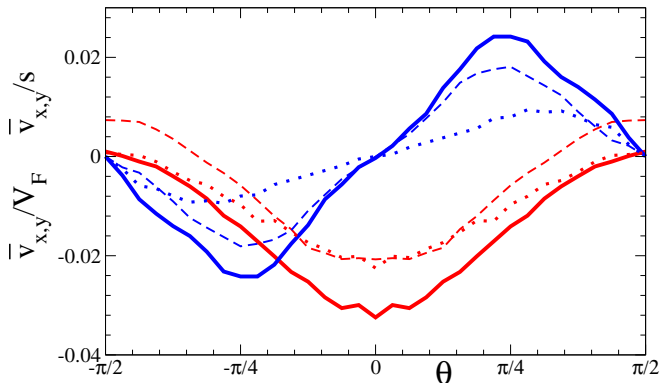


Fig. 5. (Color online) Polarization dependence of ratchet velocity in x (red/gray curves) and y (blue/black curves) directions. Data for graphene are taken at $fr_d/E_F = 0.2$ and $T/E_F = 0.02$ (full curves), 0.3 (dotted curves). Data for 2DEG are shown for $fr_d/E_F = 0.2$ and $T/E_F = 0.02$ (dashed curves). Other parameters are as Fig. 1.

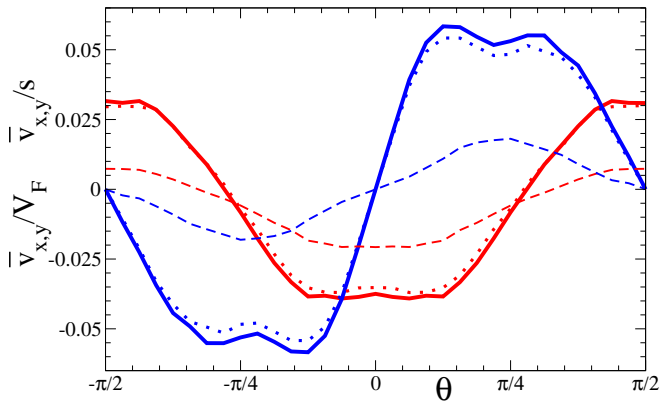


Fig. 6. (Color online) Polarization dependence of ratchet velocity in x (red/gray curves) and y (blue/black curves) directions. Data for model graphene are taken at $fr_d/E_F = 0.05$ and $T/E_F = 0.02$ (full curves), 0.3 (dotted curves). Data for 2DEG are shown for $fr_d/E_F = 0.2$ and $T/E_F = 0.02$ (dashed curves). Other parameters are as Fig. 1.

is interesting that in the case of graphene even unpolarized radiation gives an average current along x -direction with $\bar{v}_x < 0$. This is different from 2DEG case where for semidisks there is no directed current for unpolarized radiation [15]. We attribute this to the fact that for graphene $P(E)$ becomes energy dependent that acts in a similar way when scattering time $\tau(E)$ is energy dependent and when even unpolarized radiation creates a directed transport [15].

The important theoretical task is to understand the origin of a slow decrease of ratchet velocity with f for model graphene while for the graphene case the dependence remains quadratic as for 2DEG. We argue that this is due to the linear dispersion law for graphene which drastically modify the dependence of velocity \mathbf{v} on momentum and force. Indeed, in absence of collisions and impurities we have $\mathbf{v} = (\mathbf{p}_0 + \mathbf{f}/\omega \sin \omega t)/m$ where \mathbf{p}_0 is initial momentum. Thus a small force gives only a small oscillating component of velocity and thus the ratchet flow appears

only in a second order perturbation theory being proportional only to f^2 [15]. The situation is strongly different for model graphene. In absence of collisions and impurities we obtain from (1) $\mathbf{v} = s(\mathbf{p}_0 + \mathbf{f}/\omega \sin \omega t)/|(\mathbf{p}_0 + \mathbf{f}/\omega \sin \omega t)|$. Thus even for small force we have a large variation of velocity direction being of the order of radian for $|\mathbf{p}_0| \sim f/\omega$. These direction variations have many frequency harmonics in contrast to 2DEG. In presence of semidisk asymmetry and relaxation such oscillations should create a directed transport with ratchet velocity $\bar{v} \sim s$. However, in the Fermi-Dirac distribution the fraction w of electrons with such small momenta $p_0 < f/\omega$ is $w \sim fs/(\omega E_F) \sim fr_d/E_F$, where we took into account that in the case of small ω the collisions with semidisks will restrict the length s/ω by a length proportional to r_d . These arguments lead to the ratchet velocity $\bar{v} \sim sw \sim sfr_d/E_F$ being compatible with the dependence (4) found numerically. According to them a physical origin of slow decrease of \bar{v} with f is related to linear dispersion and Dirac singularity in graphene. In such a case electrons with momentum $p \ll p_F$ still have a large velocity s and give a large contribution to the ratchet flow in contrast to 2DEG.

It is interesting to note that at high frequencies ω only few collisions happen during a period of oscillations so that in average we have $\langle |\mathbf{p}| \rangle \approx \sqrt{p_0^2 + f^2/2\omega^2}$ that looks like an appearance of effective mass at large f . This mass effectively drives the system to a situation similar to 2DEG given a reduction of \bar{v} at large f (see black dashed curve in Fig. 2 inset).

The above arguments attribute the strong ratchet transport to contribution of trajectories in a vicinity of Dirac critical point in the model graphene. In this model the measure $P(E)$ of such trajectories is independent of energy $E \rightarrow 0$. However, for real graphene this measure drops with energy $P(E) \propto E$ and therefore the contribution of this region gives a weaker quadratic dependence on the driving force f that is compatible with the numerically established dependence (5). The numerical factor C_g is larger than in 2DEG but the enhancement of ratchet transport is not so strong as for model graphene.

The electron current produced by ratchet flow is given by relation $j = en_e \bar{v}$. According to (3),(5) we have for 2DEG

$$j_F \approx 0.4en_e V_F (fr_d/E_F)^2 \approx J_F (n_0/n_e)^{1/2} (fr_d/1K)^2, \quad J_F \approx 4 \cdot 10^{-5} A/cm; \quad (6)$$

and for graphene

$$j_g \approx 1.3en_e s (fr_d/E_F)^2 \approx 1.3e(fr_d)^2/\pi s \hbar^2 \approx J_g (fr_d/1K)^2, \quad J_g \approx 1.5 \cdot 10^{-5} A/cm; \quad (7)$$

where we normalize data in respect to typical parameters of 2DEG in [13] with $n_0 = 2.5 \cdot 10^{11} cm^{-2}$, $m = 0.067m_e$, $f/e = 1V/cm$, $r_d = 1\mu m$, $fr_d \approx 1K$, $E_F \approx 100K$, $V_F \approx 2.2 \cdot 10^7 cm/s$ and usual parameters of graphene $s \approx 10^8 cm/s$ [3,5]. It is interesting that for graphene the ratchet current is independent of electron density n_e (we use the relation $n_e = p_F^2/\pi \hbar^2$ [3]).

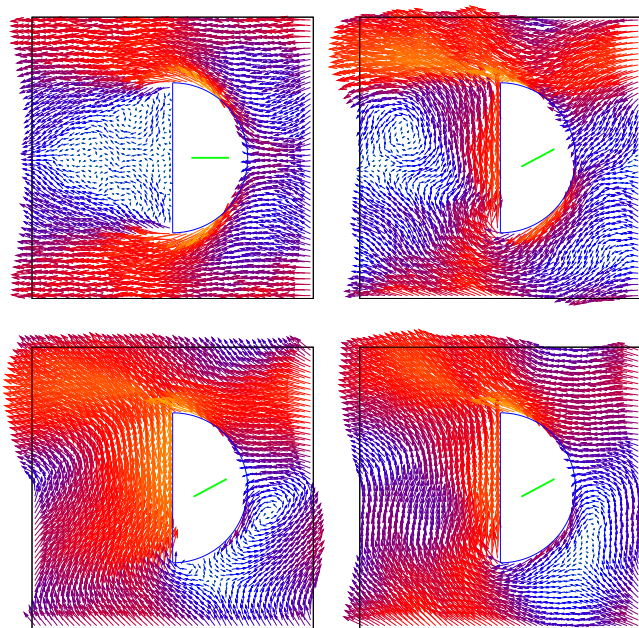


Fig. 7. (Color online) Map of local averaged velocities inside one cell in plane (x, y) for graphene at $\theta = 0$ (top left panel) and $\theta = 5\pi/32$ (top right panel) with parameters of Fig. 5; for model graphene at $\theta = 5\pi/32$ (bottom left panel) and parameters of Fig. 6; for 2DEG at $\theta = 5\pi/32$ (bottom right panel) and parameters of Fig. 5; polarization is shown by bar inside semidisk. The velocities are shown by arrows which size is proportional to the velocity amplitude, which is also indicated by color (from large (yellow/gray) to small (blue/black) amplitudes).

The comparison of estimates for 2DEG (6) and graphene (7) show that the ratchet currents in these two materials have comparable values. Of course, the above Eqs. (6),(7) assume that the mean free path in graphene is larger than the semidisk radius $r_d \sim 1\mu m$. For 2DEG the mobility drops significantly with increase of temperature and the ratchet transport disappears according to theory at small mean free path [15] and according to experimental results presented in [13]. For 2DEG the experiments [13] show that the ratchet transport at such r_d values persists only up to $T \approx 70K$ while at room temperature the mean free path becomes smaller than semidisk size and the ratchet effect disappears. According to experiments with suspended monolayer graphene [5,6] the mean free path can be larger than $r_d \sim 1\mu m$ at room temperature so that the graphene ratchet transport should be well visible at room temperature. At present it is possible to realize large size samples with epitaxial graphene [26,27] and chemical vapor deposition [28] with room temperature mobility of $20000cm^2/Vs$. For graphene even at room temperature the mean free path can be rather large and thus the ratchet transport can be significant even at room temperature. For strong microwave fields of $10V/cm$ ratchet currents can be of the order of $10^{-3}A/cm$.

In conclusion, our theoretical studies show that graphene ratchet transport in asymmetric antidot arrays, at micron

antidot size, should be well visible at room temperature in contrast to the case of 2DEG. This shows that such graphene structures can have future promising applications for simple room temperature sensors of microwave and terahertz radiation. A decrease of antidot size can make such structures to be sensitive to infrared radiation with possible photovoltaic applications.

We thank A.D.Chepelianskii for useful discussions and for pointing to us promising properties of graphene [4,5,6] for ratchet transport. We also thank M.V.Entin and L.I.Magarill for critical remarks. This work is supported in part by ANR PNANO project NANOTERRA.

References

1. K.S. Novoselov, A.K. Geim, S.V. Morozov, D. Jiang, Y. Zhang, S.V. Dubonos, I.V. Grigorieva, and A.A. Firsov, *Science* **306**, 666 (2004).
2. A.K. Geim and P. Kim, *Sci. Am.* **298**, 90 (2008).
3. A.H. Castro Neto, F. Guinea, N.M.R. Peres, K.S. Novoselov, and A.K. Geim, *Rev. Mod. Phys.* **81**, 109 (2009).
4. S.V. Morozov, K.S. Novoselov, M.I. Katsnelson, F. Schedin, D.C. Elias, J.A. Jaszczak, and A.K. Geim, *Phys. Rev. Lett.* **100**, 016602 (2008).
5. K.I. Bolotin, K.J. Sikes, Z. Jiang, M. Klima, G. Fudenberg, J. Hone, P. Kim, and H.L. Stormer, *Solid St. Comm.* **146**, 351 (2008).
6. X. Du, I. Skachko, A. Barker, and E.Y. Andrei, *Nature Nanotech.* **3**, 491 (2008).
7. F. Jülicher, A. Ajdari, and J. Prost, *Rev. Mod. Phys.* **69**, 1269 (1997).
8. R.D. Astumian and P. Hänggi, *Physics Today* **55** (11), 33 (2002).
9. P. Reimann, *Phys. Rep.* **361**, 57 (2002).
10. A. Lorke, S. Wimmer, B. Jäger, J.P. Kotthaus, W. Wegscheider, and M. Bichler, *Physica B* **249-251**, 312 (1998).
11. H. Linke, T.E. Humphrey, A. Löfgren, A.O. Sushkov, R. Newbury, R.P. Taylor, and P. Omling, *Science* **286**, 2314 (1999).
12. A.M. Song, P. Omling, L. Samuelson, W. Seifert, I. Shorubalko, and H. Zirath, *Appl. Phys. Lett.* **79**, 1357 (2001).
13. S. Sassine, Y. Krupko, J.-C. Portal, Z. D. Kvon, R. Murali, K.P.Martin, G.Hill, and A.D.Wieck, *Phys. Rev. B* **78**, 045431 (2008).
14. A.D. Chepelianskii, *Eur. Phys. J. B*, **52**, 389 (2006).
15. A. D. Chepelianskii, M. V. Entin, L. I. Magarill and D. L. Shepelyansky, *Eur. Phys. J. B* **56**, 323 (2007).
16. A. D. Chepelianskii, M. V. Entin, L. I. Magarill and D. L. Shepelyansky, *Phys. Rev E* **78**, 041127 (2008).
17. F. Galton, *Natural Inheritance* (Macmillan, London, 1889).
18. I.P. Kornfeld, S.V. Fomin, and Y.G. Sinai, *Ergodic theory* (Springer, Berlin, 1982).
19. C. Ojeda-Aristizabal, M. Monteverde, R. Weil, M. Ferrier, S. Guéron, and H. Bouchiat, *Phys. Rev. Lett.* **104**, 186802 (2010).
20. M.V.Entin, L.I.Magarill, and D.L.Shepelyansky, *Phys. Rev. B* **81**, 165441 (2010).

21. J. Karch, P. Olbrich, M. Schmalzbauer, C. Brin-
steiner, U. Wurstbauer, M.M. Glazov, S.A. Tarasenko,
E.L. Ivchenko, D. Weiss, J. Eroms, and S.D. Ganichev,
arXiv:1002.1047 (2010).
22. S. Mai, S.V. Syzranov, and K.B. Efetov, arXiv:1010.3618
(2010).
23. G. Carapella and G. Costabile, Phys. Rev. Lett. **87**, 077002
(2001).
24. M. Beck, E. Goldobin, M. Neuhaus, M. Siegel, R. Kleiner,
and D. Koelle, Phys. Rev. Lett. **95**, 090603 (2005).
25. V.M. Biryukov, Y.A. Chesnokov, and V.I. Kotov, *Crystal
Channeling and its Application at High-Energy Accelerators*,
Springer, Berlin (1997).
26. C. Berger, Z. Song, X. Li, X. Wu, N. Brown, C. Naud,
D. Mayou, T. Li, J. Hass, A.N. Marchenkov, E.H. Conrad,
P.N. First, and W.A. de Heer, Science **312**, 1191 (2006).
27. W.A. de Heer, C. Berger, X. Wu, M. Sprinkle, Y. Hu,
M. Ruan, J.A. Stroscio, P.N. First, R. Haddon, B. Piot,
C. Faugeras, M. Potemski, J.-S. Moon, arXiv:1003.4776
(2010).
28. X. Li, C.W. Magnuson, A. Venugopal, E.M. Vogel,
R.S. Ruoff, and L. Colombo, arXiv:1010.3903 (2010).